



## COMPARISONS OF MEASURED AND PREDICTED PAVEMENT STRAIN IN FULL-SCALE ACCELERATED PAVEMENT TESTING

Dae-Wook Park<sup>1</sup>, In-Tai Kim<sup>2</sup>

<sup>1</sup>Dept of Civil Engineering, Kunsan National University, San 68 Miryong-dong,  
Kunsan, Chellabuk-do, 573-701, Korea

<sup>2</sup>Dept of Transportation Engineering, Myongji University, San 38-2 Nam-Dong, Chein-Gu, Youngin,  
Kyunggi-do, 449-728, Korea

E-mails: <sup>1</sup>dpark@kunsan.ac.kr; <sup>2</sup>kit1998@mju.ac.kr

**Abstract.** In this paper, the measured and predicted responses between a full-scale accelerated pavement test facility and that from a three-dimensional (3D) finite element model were compared using the measured 3D tire contact stresses. The objective was to predict pavement response in asphalt mixture layers using the measured 3D tire contact stresses and compare with the measured transverse strains in August and November. To carry out this objective, the transverse strains within asphalt layers were measured and the corresponding strains were predicted by 3D finite element analysis. Additionally, a layered elastic analysis, the BISAR program, was used to predict the corresponding field measurements. The predicted transverse strains by 3D finite element analysis were matched reasonably with the measured strains.

**Keywords:** accelerated pavement testing, tire contact stress, finite element model (FEM), pavement response.

### 1. Introduction

As high speed computers have evolved and researchers in the area of pavement performance have become increasingly interested in the simulation of more realistic pavement structures and loading conditions, interest in the modelling of pavement structures by finite element methods (FEM) has rapidly grown. Also, as advanced measurement techniques of tire contact stresses have been developed, recent studies found that vertical tire contact stress is neither uniform nor circular and is higher than tire inflation pressure (Al-Qadi *et al.* 2008; De Beer *et al.* 1997; Marshek *et al.* 1986; Myers *et al.* 1999; Wang, Roque 2010).

Al-Khateeb *et al.* (2007) conducted a mechanistic analysis of asphalt pavements under an accelerated loading facility (ALF). Multilayer elastic theory (MLET) solutions, finite element (FE) analysis, and analysis using the VESYS 5W program were used for the predictions of the primary responses. The predicted responses included the horizontal tensile stress and strain for the fatigue mode at the bottom of the hot mix asphalt layer and the vertical compressive stresses and strain on the top of each pavement layer on the rutting mode. Their solutions of the MLET that used a linear elastic base and the VESYS 5W

programs have provided reasonable predictions that are comparable with measured tensile strains and permanent vertical deformations.

Willis and Timm (2008) made an investigation on establishing the practical level of between-gauge precision for measurements of asphalt strain under a full-scale dynamic load testing at the National Center for Asphalt Technology Pavement Test Track. They have found in their investigations that there was less variability between the gauge measurements in the longitudinal strain than the transverse strain. Least differences in strain were found at the steer axles, followed by the tandem and trailing axles. They also concluded that the measured differences in strain gauge measurements could be significantly related to the condition of the pavement.

Park *et al.* (2008a) conducted a study of the effects on the predicted transverse and vertical strains by tire load and inflation pressure. A database of measured tire contact stresses were used in interpolating 3D tire contact stresses of six different tires. The predicted transverse and vertical strains in the pavement structures were investigated by a 3D FE analysis that can apply 3D tire contact stresses. When the tire inflation pressure was increased, the results show that the predicted strains were different near the asp-

halt concrete layer. Similarly, predicted values of strain at the base and subgrade layer were different under an increased tire load. It was concluded from a statistical analysis that different asphalt concrete (AC) thicknesses, AC moduli, and subgrade moduli affected the predicted transverse strains at the bottom of asphalt layer and vertical strains at the top of subgrade.

Luo and Prozzi (2007) made an evaluation of the effects on the pavement response of the measured three-dimensional (3 D) tire-pavement contact stress that are non-uniformly distributed at the asphalt surface. Five wheel loads, five tire inflation pressures, and 12 pavement structures were evaluated using the multilayer linear elastic computer program CIRCLY. The program has the ability to handle normal and shear stresses at the pavement surface and predicted responses were the horizontal strains in the longitudinal and transverse directions. With a non-uniform contact stress distribution, results from the studies show that horizontal strains at the pavement surface are compressive within the contact area and tensile at the edge of or outside the contact area. They further concluded that the vertical and transverse contact stress have significant effects on the longitudinal strains.

Molenaar (2004) found that top-down cracking is due to shear stresses in longitudinal and transverse directions in reality, and simple vertical uniform stresses too simple to develop tensile strain at the surface of pavement layer.

Wang and Al-Qadi (2009) predicted stress and strains in the pavement using uniform stress and a 3D tire contact stress at various loading levels. The study results showed that uniform stress could underestimate the pavement damage at the pavement near surface. The difference of pavement response between uniform and 3D measured contact stresses was decreased when wheel load increases.

Greene *et al.* (2010) conducted a study on the damage by dual tires (11R22.5) and super single wide base tires (425/65R22.5, 445/65R22.5 and 455/65R22.5). Accelerated pavement testing as well as theoretical modelling was conducted to evaluate pavement damage. The study results revealed that a single wide base tire has more damage impact than dual tires.

Comparisons between the predicted response at the bottom of asphalt layer or at the top of subgrade were the focus of most of the earlier researches by different prediction methods without verifying the quantity and trend of the measured pavement response. The objective of this research was to compare the measured transverse strains at the different depths with the predicted transverse strains by the 3D FE analysis and a layered elastic program. In this paper, the influence of 3D tire contact stresses on predicted transverse strains at the center of loading, and at a 100 cm offset from loading were investigated by the authors using the 3D FE program to model the response of an asphalt pavement section located within the Korea Highway Cooperation (KHC) test road. The measured transverse strains at 5 cm, 12 cm, 20 cm and 30 cm from instrumented field tests were compared with the corres-

ponding results from 3D FE and layered elastic analyses. The analysis variables included:

- two different weather conditions (August and November 2004);
- two different vehicle speeds (30 km/h and 80 km/h);
- 3D FE analysis using measured 3D contact stresses;
- BISAR analysis using measured tire contact areas to determine equivalent uniform circular pressure distributions (referred to as the BM analysis in this paper);
- BISAR using the conventional procedure of calculating the equivalent circular loaded area by dividing the tire load with the tire inflation pressure (BC analysis).

## 2. Korea Highway Cooperation test road

### 2.1. Descriptions of test road

The KHC test road is a full-scale accelerated pavement test facility. This facility has been trafficked since March 2004. Its main purpose is to provide guidelines for application of the Korea Pavement Design Guide. The KHC test road is a 7.7 km long two-lane expressway with 33 AC and 25 Portland cement concrete sections. The AC pavement sections are composed of the AC surface layer, AC binder layer, AC treated base layer, crushed stone subbase layer and frost-resistance layer on the top of the subgrade. The thicknesses of the surface layer and binder layer are 5 cm and 7 cm, respectively, for all the AC sections while the thickness of asphalt base (8 cm, 18 cm and 28 cm) and the type of base material (25 mm and 40 mm AC-treated, and aggregate) were used as design variables. Section A5, which was used in this study, has an AC surface course of 5 cm, AC binder course of 7 cm, AC base of 18 cm, crushed stone subbase of 30 cm, and a frost-resistance layer of 30 cm on top of the subgrade. The transverse strain gauge used in this study is KM-100-HAS made by Tokyo Sokki Kenkyujo Company and the precision is 3% of measured strain. Four sets of six strain gauges at the bottom of the surface layer, binder layer, and base layer, and at mid-depth of the base layer were installed in the test section to record dynamic strain response to loads at different depths (5 cm, 12 cm, 20 cm and 30 cm) as shown in Fig. 1.

### 2.2. Measurements of strain

Section A5 was selected to investigate effects of vehicle speeds and seasonal temperatures on the strain variation within the asphalt pavement layers. Eight strain gauges at the ASG 4 and ASG 6 locations were used to investigate pavement transverse strain response to loading. The transverse strains due to the wheel of the steering axle on the driver's side were investigated as the largest strains were observed under the steering axle. As shown in Fig. 2, the effects of temperatures on the transverse strains are significant at both locations (ASG 6 and ASG 4). The transverse strains at 30 km/h in August were a little bit larger than the strains measured in the same month at 80 km/h under the

center of loading (ASG6). The difference between transverse strains diminished 100 cm from the center of loading. The effects of vehicle speed on the transverse strains measured at both locations were not significant based on data collected in November.

Measurements for the compressive transverse strain under the center of loading were taken at the bottom of the AC surface layer. At ASG4, tensile strains were measured at the same depth. Generally speaking, the measured pavement strains were significantly affected by differences in pavement temperature when comparing results from August and November 2004.

### 3. Tire contact stress

#### 3.1. Equipment and tire used in this study

An 11R22.5 tire was used to apply loading in KHC test road. At a tire load of 28.84 kN and inflation pressure of 896 kPa, the largest transverse strains were found at the driver's side wheel of the steering axle with single tire. The Tire View computer program for estimating tire contact pressure distributions in the longitudinal, lateral, and vertical directions was used to obtain the tire contact stresses, where the measurements of tire contact stresses were not available at this particular loading condition (Park *et al.* 2008b). The type, inflation pressure, and load on a tire are among the input values for the Tire View program. A database of measured tire contact pressures from tests conducted using an improved version of the VRSPATA known as the SIM Mk IV was used by the program as an interpolation routine. In a previous study, Park *et al.* (2005) presented relationships for predicting tire contact areas developed from tire imprints taken from tests performed during the TTI project. The tire imprints were digitized and a program was then used to read the electronic prints and to calculate the contact area based on the shading intensity of the pixels read. The relationships between tire load, tire

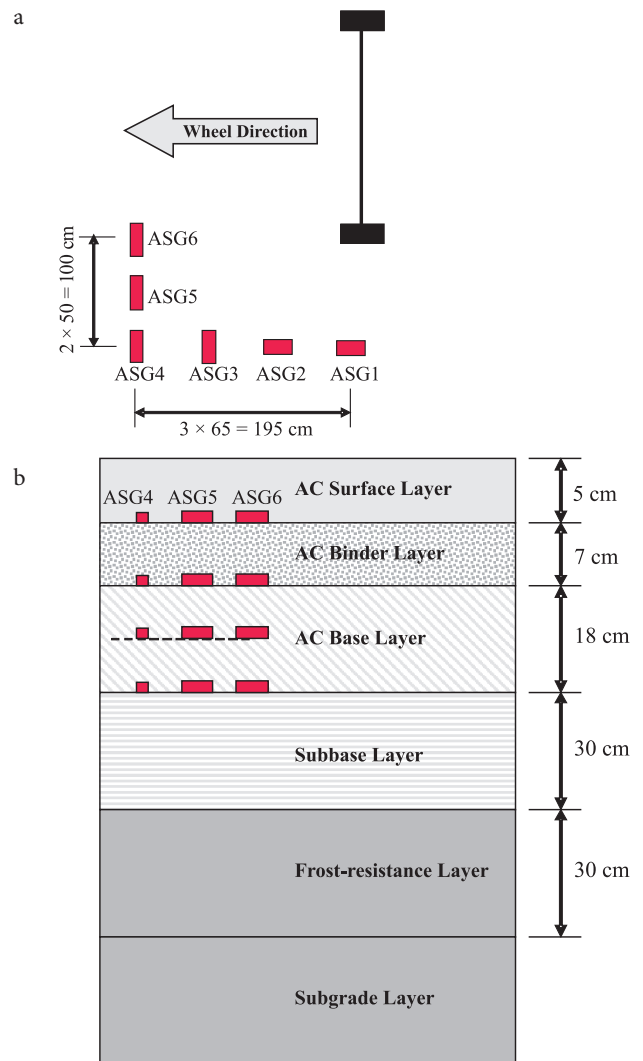


Fig. 1. Test section A5: a – plan view of instrumentation schematic; b – vertical view of strain gauge locations and pavement thickness

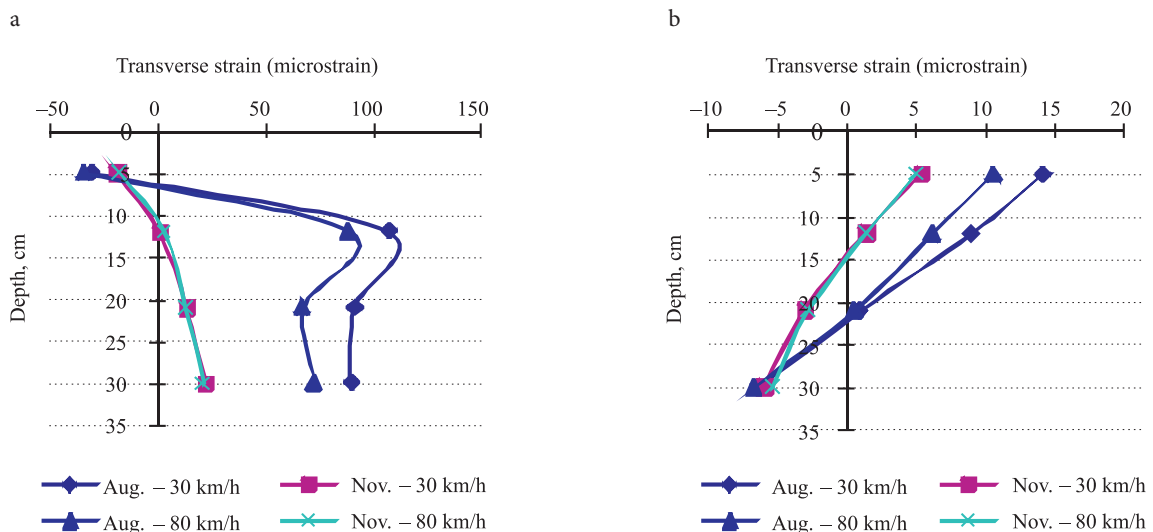


Fig. 2. Measured transverse strain for: a – ASG 6; b – ASG 4

inflation pressure and tire contact area were determined by regression analysis for the different tires tested. For the 11R22.5 radial tire, the equation to predict the tire contact area is given by the Eq:

$$A = 54.4740 + 0.0066 \times T_L - 0.4258 \times T_p,$$

where  $A$  – predicted tire contact area, in<sup>2</sup> (= 645.16 mm<sup>2</sup>);  $T_L$  – tire load, lbs (= 4.448 N);  $T_p$  – tire inflation pressure, psi (= 6.895 kPa).

### 3.2. Analysis of tire contact stresses

The contact forces in X, Y, and Z directions were obtained from the output file of Tire View. Researchers then computed the contact stresses by dividing the contact forces by the effective area of each load pin (= 250.26 mm<sup>2</sup>).

In previous study (Park *et al.* 2005) measurements were taken along the longitudinal direction for the tire contact stresses at approx 2-mm intervals for the 11R22.5 tire. In a 3D FE analysis, these fine measurements cannot be directly used. Researchers used a simple routine to reduce the sampling rate to reduce computation time to a feasible level without significant loss of accuracy. This process is called decimation because the original data sample

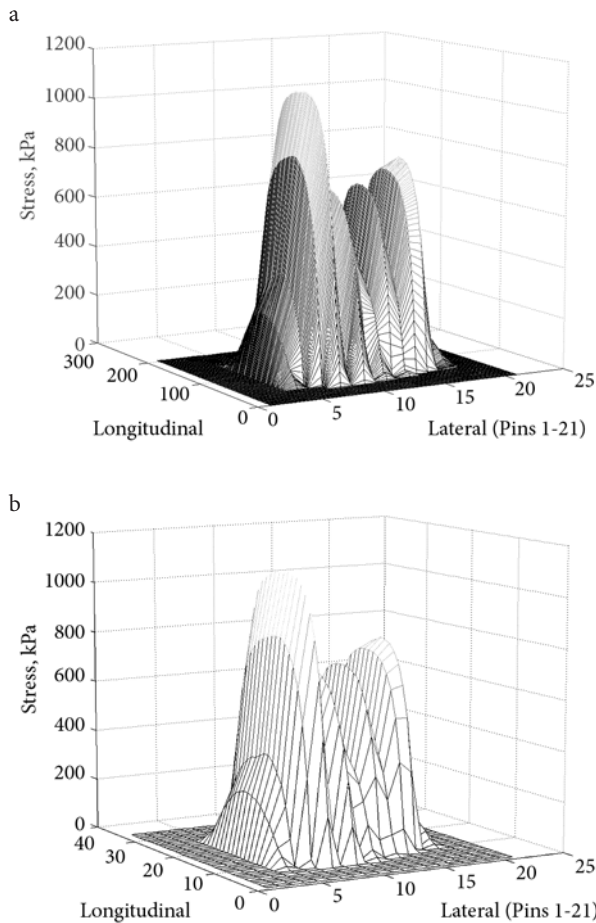


Fig. 3. Tire contact stress in vertical direction: a – original data; b – decimated data

is decreased (Stearns, Ruth 1992). A procedure for decimation is accomplished that preserves the frequency content of the original data using a finest mesh size configuration of approx 10 mm in the direction of wheel travel. The decimated tire contact stresses for an 11R22.5 radial tire corresponding inflated to 896 kPa and loaded to 28.8 kN is compared to the original tire contact stresses from Tire View as shown in Fig. 3.

## 4. Analysis methods

### 4.1. 3D FEM

The multi-purpose FE package, ABAQUS, was used to establish a 3D FE model. For predicting pavement response under measured tire contact stresses, a suitable mesh configuration had to be initially determined. Several mesh configurations of varying numbers of elements and element types, and which are horizontally infinite and vertically semi-infinite, were evaluated by comparing FE predictions with corresponding predictions from the BISAR program. The FE mesh was varied in the lateral and longitudinal dimensions until the FEM and layered elastic analysis predictions of pavement response compared reasonably well. An appropriate FE mesh with lateral dimension of 3.81 m and longitudinal dimension of 3.81 m was determined from this analysis, and where infinite elements were used to model the subgrade.

The tire contact area consisted of 20 columns and 34 rows of elements that are approx 17 mm (column) × 10 mm (row) in size, used to model the region of the tire contact stresses. A coarser mesh was used outside of the wheel load area, with the element size progressively increasing with distance from the load. With this biased mesh configuration, computation time was reduced. The interface between layers was assumed to be fully bonded. To verify the 3D FEM, the predicted transverse horizontal strains by 3D FEM and BISAR under the same uniform loading condition were compared as shown in Fig. 4.

### 4.2. Layered elastic analysis

In this analysis, the results from the measured horizontal strains with corresponding predictions from the layered

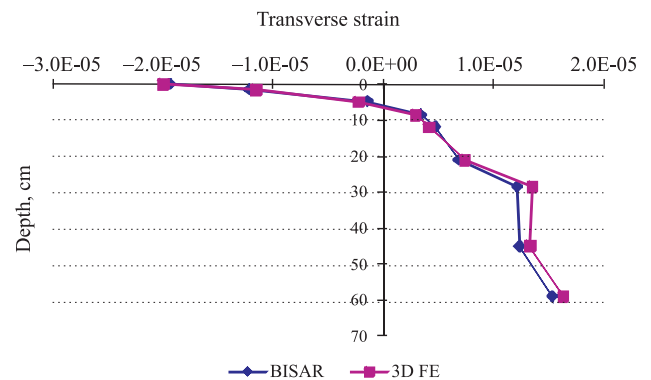


Fig. 4. Validation of the 3D FEM

elastic analysis were compared. Two types of layered elastic analysis were used as noted earlier in the paper. Equation was used to calculate the measured tire contact area for the 11R22.5 tire in the BM analysis, and the area was used to calculate an equivalent uniform circular pressure distribution. In the case of the conventional (BC) analysis, the tire contact area and its radius were determined based on load divided by the tire inflation pressure. In the conventional analysis, the tire inflation pressure is assumed as the tire contact stress on the pavement surface. The input data for the BISAR program are summarized in Table 1.

**Table 1.** Summary of input data for BM and BC analysis

Type of analysis		BISAR with measured contact area (BM)	BISAR with conventional method (BC)
Given data	Load, kN	28.4	28.4
	Pressure, kPa	896	896
	Area, mm <sup>2</sup>	26 613	31 684
Input data for BISAR	Pressure, kPa	1068	896
	Radius, mm	19.55	21.33

### 4.3. Material properties

In the analysis, dynamic modulus was used as a material property to consider different loading frequencies and temperatures. The dynamic modulus tests were conducted at four different temperatures (−10 °C, 10 °C, 35 °C and 54 °C) and eight different loading rates (0.01 Hz, 0.05 Hz, 0.1 Hz, 0.5 Hz, 1 Hz, 5 Hz, 10 Hz and 25 Hz) using lab-mixed and lab-compacted specimens. From the test data, the authors generated master curves for the asphalt mixtures used in the AC surface, AC binder, and AC base layers of the section investigated in this paper. Temperature gauges were installed at the mid-depth of each asphalt layer to collect temperature data during loading applications. The average measured temperature in August and November from 9:00 AM to 6:00 PM was shown in Fig. 5.

The dynamic moduli of each asphalt layer at different temperatures and vehicle speeds was calculated using the corresponding master curve for each material. The master curves of the AC layers at 10 °C are shown in Fig. 6. The modulus of the subbase layer, freeze-resistant layer, and subgrade were backcalculated using MODULUS 5.0 based on the deflection measurements by falling weight deflectometer tests. Typical values of Poisson’s ratio for all the layers were assumed corresponding to the materials found in the road test sections based on data reported in the literature (Huang 1993). Table 2 summarizes the elastic moduli and Poisson’s ratios used in this analysis. From this table, the dynamic modulus of the surface layer is observed to be smaller than that of the binder and base layers.

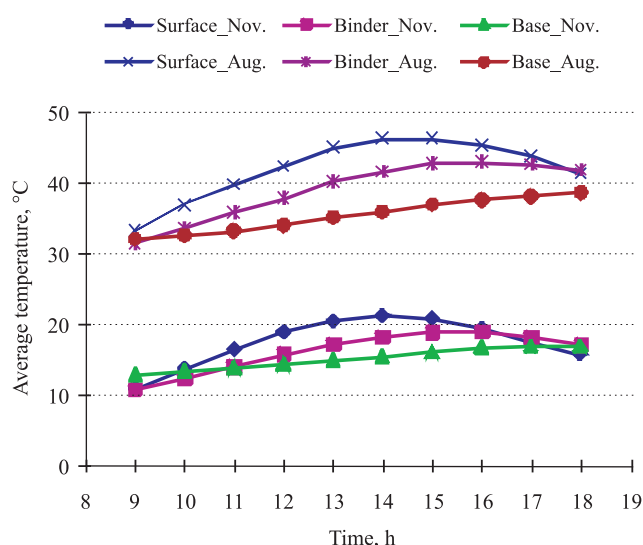


**Fig. 5.** Average measured temperature in August and November, 2004

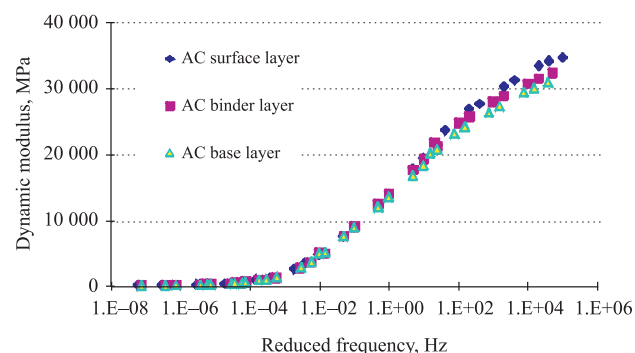


**Fig. 6.** Dynamic modulus at 10 °C reference temperature

## 5. Prediction of pavement responses

### 5.1. Predicted transverse strains

The predicted transverse strains of asphalt layers from the 3D FE analysis were compared with the results of instrumented field tests. The transverse strains were predicted using different dynamic AC moduli corresponding to the temperatures and vehicle speeds considered in this investigation. Inputs to the 3D FE model were the 3D tire contact stresses in the longitudinal, lateral and vertical directions. The measured transverse strains at ASG6 and ASG4 were predicted and these predictions with the measured values were compared.

The equivalent uniform circular contact stresses for the 11R22.5 radial tire, based on the measured tire contact areas, are larger than the tire inflation pressures, which are used as contact stresses in the conventional layered elastic (BC) analysis as shown in Table 2. Thus, the predicted transverse strains from the modified layered elastic (BM) analysis are observed to be slightly higher than the corresponding predictions from the BC analy-

sis in the upper pavement layer. The predicted tensile strains in the binder layer from layered elastic analysis are higher than the corresponding predictions from the 3D FE analysis.

**5.2. Comparisons of measured and predicted transverse strains**

Comparisons between the measured and predicted transverse strains were made for the purpose to investigate the effects of the 3D tire contact stresses that were measured, rather than comparing the prediction capacity by three prediction methods which have elastic material property. Therefore; the shape of predicted strains with depth as well as the quantity of predicted strains was compared.

As transverse strains were measured at the center of loading (ASG6) and at a 100 cm offset from the center (ASG4), the measurements at these two locations were compared to the predicted strains from the three analysis methods. A total of four cases (30 km/h in August, 80km/h in August, 30 km/h in November and 80 km/h in November) were compared. As shown in Fig. 1b, the transverse strains at four different locations (5 cm, 12 cm, 20 cm, and 30 cm from the top of surface) were predicted using the 3D FE, BM and BC methods.

Fig. 7 compares the predicted transverse strains with the measured values at ASG6 and ASG4 in August. The results show that the large discrepancies exist under the center of loading (ASG6 strain gauges) between the measured transverse strains and predicted transverse strains by all prediction methods. However, the shape of prediction curve by 3D FE analysis shows the similar trend. For instance, the measured and predicted transverse strains at ASG6 by 3D FE analysis are compressive at the bottom of the surface layer (depth 5 cm) while the results from the layered elastic analysis show tensile strains at the same depth.

At the bottom of surface layer, tensile strains were shown from the results of the three analysis methods as well as the measured values at ASG4. In addition, the predictions and the measurements show similar in the strain variation with depth into the pavement. Comparisons of the measured and predicted tensile strains by 3D FE analysis are closer at the bottom of surface layer for the two temperatures considered. Overall, the predicted transverse strains by 3D FE analysis show closer values and the curve shape of predicted strains shows the similar trend.

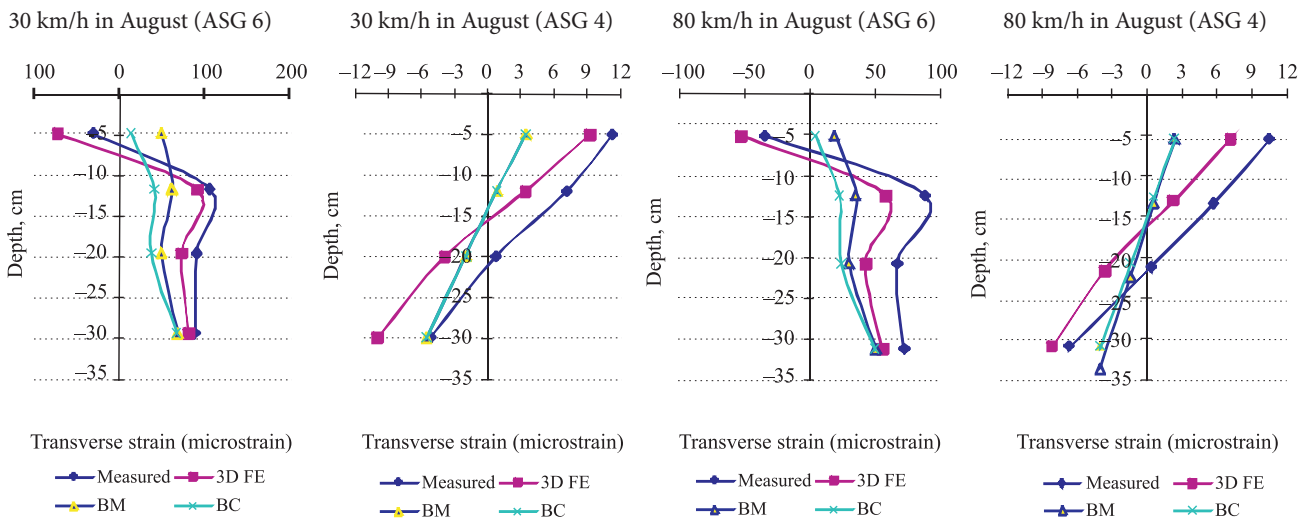
Fig. 8 compares the measured and predicted transverse strains at ASG6 and ASG4 in November. The predicted transverse strains at ASG6 by 3D FE analysis are

**Table 2.** Material property used in analysis

Season	Speed, km/h	Modulus of layer, MPa					
		AC surface	AC binder	AC base	AC subbase	FR	Subgrade
August	30	1924	2365	2696			
August	80	2944	3661	4413			
November	30	14 307	15 872	15 244	345	69	45
November	80	17 541	18 975	18 154			

Poisson's ratio						
Layer	AC surface	AC binder	AC base	AC subbase	Frost-resistance layer	Subgrade
Poisson's ratio	0.35	0.35	0.35	0.40	0.40	0.45



**Fig. 7.** Comparisons of the measured and predicted transverse strains

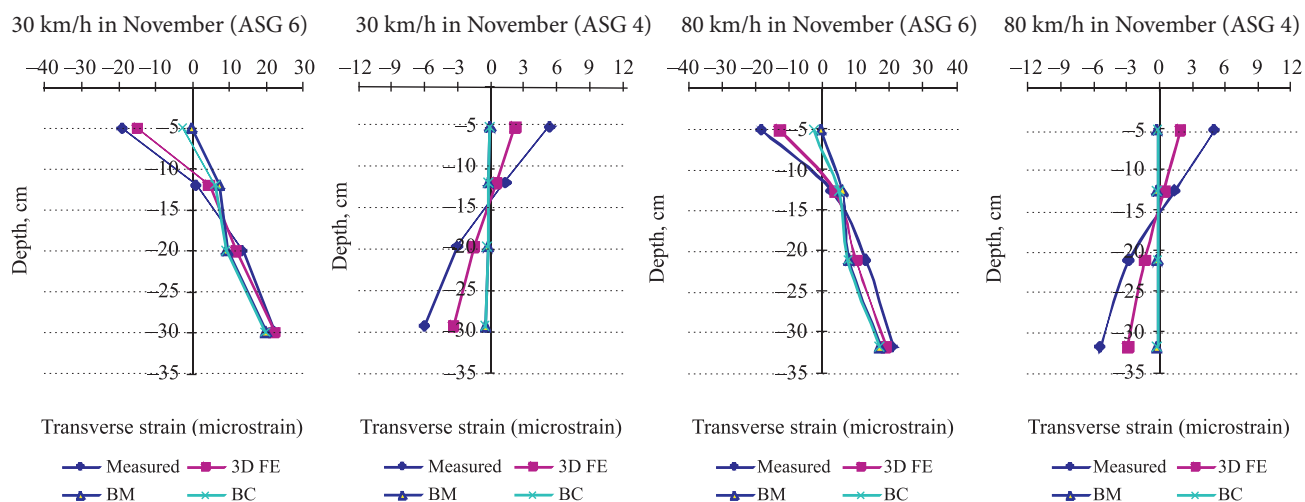


Fig. 8. Comparisons of the measured transverse strains and predicted transverse strains

very close to the measured transverse strains compared to the comparisons in August. At ASG4, the difference between the measured and predicted transverse strains show the similar compared to the comparisons in August. Overall, the shape of predicted strain curve by 3D FE analysis shows the similar trend. For instance, the measured transverse strains and the predicted transverse strains by 3D FE analysis are observed to change from tensile to compressive with depth from the bottom of the surface layer, while the predictions with BISAR are all compressive.

## 6. Conclusions and recommendations

The measured transverse strains were observed to depend on pavement temperature. Vehicle speed showed no significant effects on pavement response for the conditions under which the measurements were collected in this study. This suggests that the material property such as dynamic modulus was significantly changed by temperature rather than vehicle load frequency.

For comparisons of transverse strains measured at ASG6 in August, the predicted transverse strains by 3D FE analysis showed the similar results in terms of quantity and trend to the measured results. At the bottom of surface layer, the measured and predicted tensile strains by 3D FE analysis were closer at ASG4. Overall, the predictions and measured transverse strains at this offset location are significantly smaller than the values underneath the load (ASG6), indicating ASG4 to be the less critical location.

For comparisons between the measured and predicted transverse strain at ASG6 in November, the discrepancies were smaller compared to those of August. The results suggest that plastic strains are exist in the measured transverse strains during August while recoverable elastic strain are dominant in the measured transverse strains during November, and the discrepancies between the measured and predicted strains can be decreased using by the constitutive relations of nonlinear material property. The measured transverse strains and predicted transverse

strains by 3D FE analysis were observed to change from tensile to compressive with depth from the bottom of the surface layer, while the predictions by BISAR are all compressive. The results indicate that transverse and longitudinal stresses as well as non-uniform vertical contact stress caused the significant difference on predicted transverse strains near the pavement surface. This result cannot be achieved by a layered elastic program under the uniform contact stress that is assumed as a general approach in pavement industry.

For comparisons between the measured and predicted transverse strains at ASG 4, which is 100 cm offset distance from the center of wheel load, by three different analysis methods, the predicted transverse strain by 3D FE analysis is closer to the measured transverse strains and larger than that by the BISAR program. This result indicates that the larger transverse strain can cause the top down fatigue cracking which is the general trend of fatigue cracking near the wheel path area.

Based on conclusions mentioned above, the elastic material property has limitations to predict the pavement response at high temperatures. A 3D FE analysis using a viscoelastic or viscoplastic model is strongly recommended to achieve the adequate capacity of predictions.

## Acknowledgments

The authors would like to thank the Korea Research Foundation Grant funded by the Korean Government (MOE-HRD, Basic Research Promotion Fund) (KRF-2007-313-D00822) for the support granted to this work.

## References

- Al-Khateeb, G.; Gibson, N. H.; Qi, X. 2007. Mechanistic Analysis of FHWA's Accelerated Loading Facility Pavements: Primary Response, *Transportation Research Record* 1990: 150–161. doi:10.3141/1990-17
- Al-Qadi, I. L.; Wang, H.; Yoo, P.; Dessouky, S. H. 2008. Dynamic Analysis and In-Situ Validation of Perpetual Pavement to Ve-

- hicular Loading, *Transportation Research Record* 2087: 29–39. doi:10.3141/2087-04
- De Beer, M.; Fisher, C.; Jooste, F. J. 1997. Determination of Pneumatic Tyre/Pavement Interface Contact Stresses under Moving Loads and Some Effects on Pavements with Thin Asphalt Surfacing Layers, in *Proc of 8<sup>th</sup> International Conference on Asphalt Pavements*, Seattle, USA, 179–227.
- Greene, J.; Toros, U.; Kim, S.; Byron, T.; Choubane, B. 2010. Impact of Wide-Base Single Tires on Pavement Damage, *Transportation Research Record* 2155: 82–90. doi:10.3141/2155-09
- Huang, Y. H. 1993. *Pavement Analysis and Design*. Eaglewood Cliffs: Prentice Hall. 366 p. ISBN 655275-7.
- Luo, R.; Prozzi, J. A. 2007. Effect of Measured Three-Dimensional Tire-Pavement Contact Stress on Pavement Response at Asphalt Surface, *Transportation Research Record* 2037: 115–127. doi:10.3141/2037-11
- Marshak, K. M.; Chen, H. H.; Connell, R. B.; Hudson, R. W. 1986. Experimental Determination of Pressure Distributions of Truck Tire-Pavement Contact, *Transportation Research Record* 1070: 9–14.
- Molenaar, A. A. A. 2004. Bottom-Up Fatigue Cracking: Myth or Reality?, in *Proc of 5<sup>th</sup> International RILEM Conference*. May 5–7, 2004, Limoges, France, 275–282.
- Myers, L. A.; Roque, R.; Ruth, B. E. Drakos, C. 1999. Measurement of Contact Stresses for Different Truck Tire Types to Evaluate their Influence on Near-Surface Cracking and Rutting, *Transportation Research Record* 1655: 175–184. doi:10.3141/1655-23
- Park, D.-W.; Fernando, E.; Leidy, J. 2005. Evaluation of Predicted Pavement Response with Measured Tire Contact Stresses, *Transportation Research Record* 1919: 160–170. doi:10.3141/1919-17
- Park, D.-W.; Martin, A. E.; Jeong, J.-H.; Lee, S.-T. 2008a. Effects of Tire Inflation Pressure and Load on Predicted Pavement Strains, *The Baltic Journal of Road and Bridge Engineering* 3(4): 181–186. doi:10.3846/1822-427X.2008.3.181-186
- Park, D.-W.; Fernando, E.; Kim, H.; Kim, I.; Yoon, H. 2008b. Effects of Tire Types on Predicted Pavement Service Life, *Road Materials and Pavement Design* 9(SI): 339–357. doi:10.3166/RMPD.9HS.339-357
- Stearns, S. D.; Ruth, A. D. 1992. *Signal Processing Algorithm in Fortran and C*. Eaglewood Cliffs: Prentice Hall. 650 p. ISBN 978-0138126940
- Wang, G.; Roque, R. 2010. Three-Dimensional Finite Element Modeling Static-Pavement Interaction, *Transportation Research Record* 2155: 158–169. doi:10.3141/2155-17
- Wang, H.; Al-Qadi, I. L. 2009. Combined Effect of Moving Wheel Loading and Three Dimensional Tire Contact Stresses on Perpetual Pavement Response, *Transportation Research Record* 2095: 53–61. doi:10.3141/2095-06
- Willis, J. R.; Timm, D. H. 2008. Repeatability of Asphalt Strain Measurements under Full-Scale Dynamic Loading, *Transportation Research Record* 2087: 40–48. doi:10.3141/2087-05

Received 11 December 2008; accepted 6 October 2010